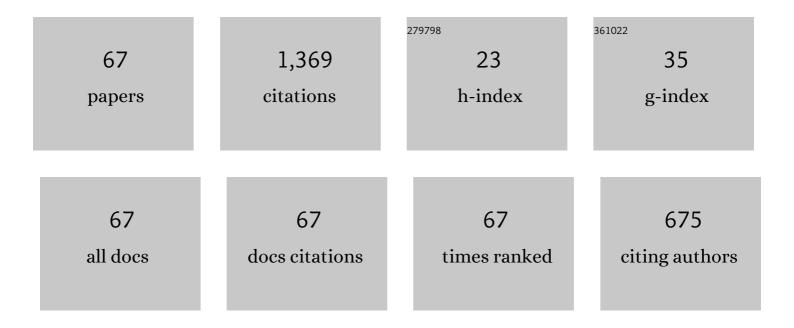
List of Publications by Year in descending order

Source: https://exaly.com/author-pdf/8313941/publications.pdf Version: 2024-02-01



#	Article	IF	CITATIONS
1	Recent Progress and Future Perspective on Mathematical Modeling of Blast Furnace. ISIJ International, 2010, 50, 914-923.	1.4	139
2	Fabrication of Self-Ordered Porous Alumina via Etidronic Acid Anodizing and Structural Color Generation from Submicrometer-Scale Dimple Array. Electrochimica Acta, 2015, 156, 235-243.	5.2	98
3	Porous Aluminum Oxide Formed by Anodizing in Various Electrolyte Species. Current Nanoscience, 2015, 11, 560-571.	1.2	64
4	Exploration for the Self-ordering of Porous Alumina Fabricated via Anodizing in Etidronic Acid. Electrochimica Acta, 2016, 211, 515-523.	5.2	61
5	Self-ordered Porous Alumina Fabricated via Phosphonic Acid Anodizing. Electrochimica Acta, 2016, 190, 471-479.	5.2	60
6	Gas–solid flow simulation of fines clogging a packed bed using DEM–CFD. Chemical Engineering Science, 2012, 71, 274-282.	3.8	44
7	Numerical Analysis of Carbon Monoxide–Hydrogen Gas Reduction of Iron Ore in a Packed Bed by an Euler–Lagrange Approach. Metallurgical and Materials Transactions B: Process Metallurgy and Materials Processing Science, 2014, 45, 2395-2413.	2.1	40
8	Polymer nanoimprinting using an anodized aluminum mold for structural coloration. Applied Surface Science, 2015, 341, 19-27.	6.1	40
9	Advanced hard anodic alumina coatings via etidronic acid anodizing. Surface and Coatings Technology, 2017, 326, 72-78.	4.8	39
10	Effect of High Reactivity Coke for Mixed Charge in Ore Layer on Reaction Behavior of Each Particle in Blast Furnace. ISIJ International, 2013, 53, 1770-1778.	1.4	37
11	Influence of Shape of Cohesive Zone on Gas Flow and Permeability in the Blast Furnace Analyzed by DEM-CFD Model. ISIJ International, 2015, 55, 1232-1236.	1.4	37
12	Mirror-finished superhydrophobic aluminum surfaces modified by anodic alumina nanofibers and self-assembled monolayers. Applied Surface Science, 2018, 440, 506-513.	6.1	37
13	Corrosion-Resistant Porous Alumina Formed via Anodizing Aluminum in Etidronic Acid and Its Pore-Sealing Behavior in Boiling Water. Journal of the Electrochemical Society, 2019, 166, C261-C269.	2.9	36
14	Superhydrophilic and superhydrophobic aluminum alloys fabricated via pyrophosphoric acid anodizing and fluorinated SAM modification. Journal of Alloys and Compounds, 2017, 725, 379-387.	5.5	34
15	DEM-SPH study of molten slag trickle flow in coke bed. Chemical Engineering Science, 2018, 175, 25-39.	3.8	30
16	Superhydrophilicity of a nanofiber-covered aluminum surface fabricated via pyrophosphoric acid anodizing. Applied Surface Science, 2016, 389, 173-180.	6.1	28
17	Model study of the effect of particles structure on the heat and mass transfer through the packed bed in ironmaking blast furnace. International Journal of Heat and Mass Transfer, 2015, 91, 1176-1186.	4.8	26
18	Detailed Modeling of Melt Dripping in Coke Bed by DEM – SPH. ISIJ International, 2018, 58, 282-291.	1.4	26

#	Article	IF	CITATIONS
19	Stable mesh-free moving particle semi-implicit method for direct analysis of gas–liquid two-phase flow. Chemical Engineering Science, 2014, 111, 286-298.	3.8	25
20	Multiphase Particle Simulation of Gas Bubble Passing Through Liquid/Liquid Interfaces. Materials Transactions, 2014, 55, 1707-1715.	1.2	25
21	SPH simulations of the behavior of the interface between two immiscible liquid stirred by the movement of a gas bubble. Chemical Engineering Science, 2016, 141, 342-355.	3.8	25
22	Analysis of Effect of Packed Bed Structure on Liquid Flow in Packed Bed Using Moving Particle Semi-implicit Method. ISIJ International, 2015, 55, 1284-1290.	1.4	25
23	A Superhydrophilic Aluminum Surface with Fast Water Evaporation Based on Anodic Alumina Bundle Structures via Anodizing in Pyrophosphoric Acid. Materials, 2019, 12, 3497.	2.9	24
24	Fabrication of ordered submicrometer-scale convex lens array via nanoimprint lithography using an anodized aluminum mold. Microelectronic Engineering, 2018, 185-186, 61-68.	2.4	23
25	Wettability Model Considering Three-Phase Interfacial Energetics in Particle Method. Materials Transactions, 2012, 53, 662-670.	1.2	20
26	Characterization of Liquid Trickle Flow in Poor-Wetting Packed Bed. ISIJ International, 2015, 55, 1259-1266.	1.4	20
27	Advancing and receding contact angle investigations for highly sticky and slippery aluminum surfaces fabricated from nanostructured anodic oxide. RSC Advances, 2018, 8, 37315-37323.	3.6	19
28	Fabrication of anodic porous alumina via galvanostatic anodizing in alkaline sodium tetraborate solution and their morphology. Journal of Electroanalytical Chemistry, 2019, 846, 113152.	3.8	18
29	Reduction of CaTiO <sub>3</sub> by Electrolysis in the Molten Salt CaCl <sub>2</sub> -CaO. Electrochemistry, 2018, 86, 82-87.	1.4	17
30	Detailed modelling of packed-bed gas clogging due to thermal-softening of iron ore by Eulerian–Lagrangian approach. Chemical Engineering Journal, 2020, 392, 123643.	12.7	16
31	An SPH Study of Molten Matte–Slag Dispersion. Metallurgical and Materials Transactions B: Process Metallurgy and Materials Processing Science, 2017, 48, 1792-1806.	2.1	15
32	Reduction of CaTiO <sub>3</sub> in Molten CaCl <sub>2</sub> - as Basic Understanding of Electrolysis. Materials Transactions, 2017, 58, 341-349.	1.2	15
33	Electrochemical and morphological characterization of porous alumina formed by galvanostatic anodizing in etidronic acid. Electrochimica Acta, 2019, 320, 134606.	5.2	15
34	Fabrication of a plasma electrolytic oxidation/anodic aluminum oxide multi-layer film via one-step anodizing aluminum in ammonium carbonate. Thin Solid Films, 2020, 697, 137799.	1.8	12
35	Spontaneous colloidal metal network formation driven by molten salt electrolysis. Scientific Reports, 2018, 8, 13114.	3.3	11
36	Capturing the nonâ€spherical shape of granular media and its trickle flow characteristics using fully‣agrangian method. AICHE Journal, 2017, 63, 2257-2271.	3.6	10

#	Article	IF	CITATIONS
37	SPH simulations of binary droplet deformation considering the Fowkes theory. Chemical Engineering Science, 2021, 229, 116035.	3.8	9
38	Recent Studies on Titanium Refining: 2017–2020. Materials Transactions, 2021, 62, 905-913.	1.2	9
39	Numerical Simulation of Coexisting Solid-liquid Slag Trickle Flow in a Coke Bed by the SPH Method with a Non-Newtonian Fluid Model. ISIJ International, 2020, 60, 1445-1452.	1.4	9
40	Morphology of lithium droplets electrolytically deposited in LiCl–KCl–Li2O melt. Electrochemistry Communications, 2017, 81, 43-47.	4.7	8
41	Column and film lifetimes in bubble-induced two-liquid flow. Physical Review E, 2018, 97, 062802.	2.1	8
42	Numerical Study of Binary Trickle Flow of Liquid Iron and Molten Slag in Coke Bed by Smoothed Particle Hydrodynamics. Processes, 2020, 8, 221.	2.8	8
43	Comprehensive numerical assessment of molten iron–slag trickle flow and gas countercurrent in complex coke bed by Eulerian–Lagrangian approach. Chemical Engineering Journal, 2021, 414, 128606.	12.7	8
44	Porous Anodic Oxide Films on Aluminum. Hyomen Gijutsu/Journal of the Surface Finishing Society of Japan, 2018, 69, 554-561.	0.2	8
45	Holdup Characteristics of Melt in Coke Beds of Different Shapes. ISIJ International, 2018, 58, 1742-1744.	1.4	7
46	Photoluminescence from Anodic Aluminum Oxide Formed via Etidronic Acid Anodizing and Enhancing the Intensity. Materials Transactions, 2020, 61, 1130-1137.	1.2	7
47	Impact of high-temperature non-uniform degradation on fines clogging and gas flow in a coke bed. Chemical Engineering Journal, 2022, 427, 131484.	12.7	7
48	Topological Consideration of 3-D Local Void Structure for Static Holdup Site in Packed Bed. ISIJ International, 2020, 60, 1453-1460.	1.4	7
49	Evaluation of Coke Degradation Effect on Flow Characteristics in Packed Bed Using 3D Scanning for Rotational Mechanical Strength Test and Solid-liquid-gas Three-phase Dynamic Model Analysis. Tetsu-To-Hagane/Journal of the Iron and Steel Institute of Japan, 2018, 104, 347-357.	0.4	7
50	Visualization of TiO2 Reduction Behavior in Molten Salt Electrolysis. Metallurgical and Materials Transactions B: Process Metallurgy and Materials Processing Science, 2020, 51, 11-15.	2.1	6
51	OS process. , 2020, , 287-313.		6
52	Solubility of CaS in CaCl <sub>2</sub> –LiCl Eutectic Melt. Materials Transactions, 2019, 60, 411-415.	1.2	5
53	Characterization of the Cathodic Thermal Behavior of Molten CaCl <sub>2</sub> and Its Hygroscopic Chloride Mixture During Electrolysis. Journal of the Electrochemical Society, 2020, 167, 102507.	2.9	5
54	Droplet behavior analysis on inclined, highly sticky, or slippery superhydrophobic nanostructured surfaces by observation and SPH simulation. Chemical Engineering Science, 2022, 248, 117214.	3.8	5

#	Article	IF	CITATIONS
55	Porous anodic oxide films on aluminum and their nanofabrication. Keikinzoku/Journal of Japan Institute of Light Metals, 2014, 64, 476-482.	0.4	4
56	Temperature Dependence of Behavior of Interface Between Molten Sn and LiCl–KCl Eutectic Melt Due to Rising Gas Bubble. Metallurgical and Materials Transactions B: Process Metallurgy and Materials Processing Science, 2016, 47, 1532-1537.	2.1	4
57	Method for Simulating Gas Permeability of a Coke Bed Including Fines Based on 3D Imaging on the Coke Particle Morphology. ISIJ International, 2021, 61, 1814-1825.	1.4	4
58	Quantification of the Impact of Residual H2O on Cathodic Behavior in Molten CaCl2 Electrolysis. Journal of Sustainable Metallurgy, 2022, 8, 532-540.	2.3	4
59	Gas Generation Reactions during TiO <sub>2</sub> Reduction Using Molten Salt. Nippon Kinzoku Gakkaishi/Journal of the Japan Institute of Metals, 2019, 83, 441-448.	0.4	3
60	Numerical Approach to Comprehend for Effect of Melts Physical Properties on Iron-slag Separation Behaviour in Self-reducing Pellet. ISIJ International, 2020, 60, 2695-2704.	1.4	3
61	Calciothermic Reduction and Electrolysis of Sulfides in CaCl2 Melt. Minerals, Metals and Materials Series, 2018, , 763-771.	0.4	2
62	Advanced functional aluminum materials based on nanostructured surface. Keikinzoku/Journal of Japan Institute of Light Metals, 2018, 68, 211-218.	0.4	2
63	Formation of Bright White Plasma Electrolytic Oxidation Films with a Uniform Maze-Like Structure by Anodizing Aluminum in Ammonium Tetraborate Solutions. Journal of the Electrochemical Society, 2022, 169, 043505.	2.9	2
64	Numerical Analysis of Interfacial Morphology and Dispersion Behavior of High-Temperature Melts. Journal of MMIJ, 2019, 135, 71-82.	0.3	1
65	Fabrication of Alumina Nanofibers via Anodizing and Its Surface Functionalization. Hyomen Gijutsu/Journal of the Surface Finishing Society of Japan, 2016, 67, 527-532.	0.2	0
66	Synchronized High-Speed Microscopy and Thermoanalytical Measurement for Sub-mm/sub-ms-scale Cathodic Behavior in Molten Salt Electrolysis. Minerals, Metals and Materials Series, 2021, , 338-345.	0.4	0
67	Numerical Analysis of Blast Furnace by Discrete Element Type Model. Japanese Journal of Multiphase Flow, 2016, 30, 166-173.	0.3	0